Electrical properties of resistive ribbon

by K. K. Shih D. B. Dove

In resistive ribbon thermal transfer printing, a printhead consisting of an array of electrodes passes current into a thin ribbon to generate heat for transferring ink to paper. The ribbon is made of a polymeric material containing carbon black so as to be conducting, and has aluminum deposited on one side of the ribbon for a base contact. In this paper, the electrical conduction processes within the ribbon are discussed. Current-voltage measurements have been made with electrodes of various types in order to separate effects due to contact resistance, aluminum/resistive ribbon interfacial resistance. and bulk conduction in the resistive ribbon. Measurements have been made over a range of frequency and temperature to determine the basic conduction mechanisms. A model of conduction is presented that is in qualitative agreement with the data.

Introduction

In resistive ribbon thermal transfer printing, a printhead consisting of an array of electrodes passes current into a thin conducting ribbon, causing it to become heated beneath the active electrodes [1, 2]. The temperature rise is sufficient that ink on the underside of the ribbon becomes molten and is transferred to a contacting sheet of paper or other material. It is important to understand both the electrical and thermal behavior of the head, ribbon, and paper if the full potential of the system is to be realized.

Copyright 1985 by International Business Machines Corporation. Copying in printed form for private use is permitted without payment of royalty provided that (1) each reproduction is done without alteration and (2) the *Journal* reference and IBM copyright notice are included on the first page. The title and abstract, but no other portions, of this paper may be copied or distributed royalty free without further permission by computer-based and other information-service systems. Permission to *republish* any other portion of this paper must be obtained from the Editor.

In this report, the electrical properties of the resistive ribbon are reviewed. The structure of the ribbon is shown in **Figure 1**. The ribbon consists of a carbon black loaded polycarbonate resistive layer 15 to 20 μ m thick, with a bulk resistivity of approximately 0.6 Ω -cm, having an aluminum layer approximately 100 nm thick deposited upon one side to act as a ground return layer for the current flowing beneath the electrodes; an ink layer is coated upon the aluminum layer.

Experimentally it is found that an electrical resistance (interfacial resistance) exists between the resistive layer and the aluminum ground plane, and that a contact resistance exists beneath the electrodes of the printhead. Due to a nonlinear conduction mechanism, the electrical resistance of the ribbon decreases as current is increased to the level required for printing.

In order to separate the effects due to the resistive layer, contact resistance, and interfacial resistance, measurements of the electrical properties have been carried out variously with deposited gold and aluminum electrodes, and with tungsten electrodes contacting the polycarbonate layer. Measurements have been made over a range of temperature, frequency, and voltage in order to understand the major conduction processes occurring within the resistive ribbon system.

Experimental details

• Sample preparation

The polycarbonate material containing 27-30% carbon black (sheet resistivity about $380~\Omega/\Box$) 15 to $20~\mu m$ thick was used as ribbon substrate material, and samples were prepared by depositing 100~nm of Al on one side as a base electrode. Similar specimens were prepared with Au as the base electrode; these were for comparison of ribbon electrical properties. After the base electrode deposition, square Au dots varying from $50~\mu m$ to $250~\mu m$ in size and 200~nm in thickness were deposited on the other side of the samples.

519

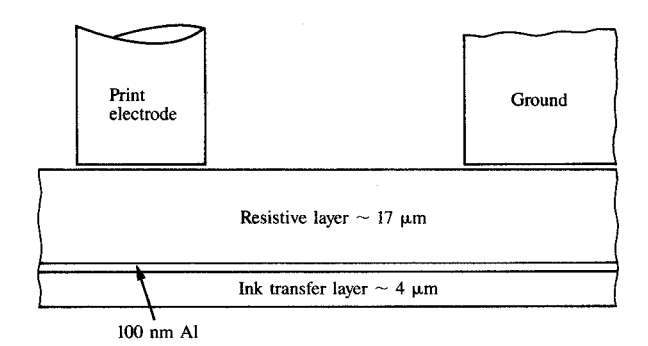
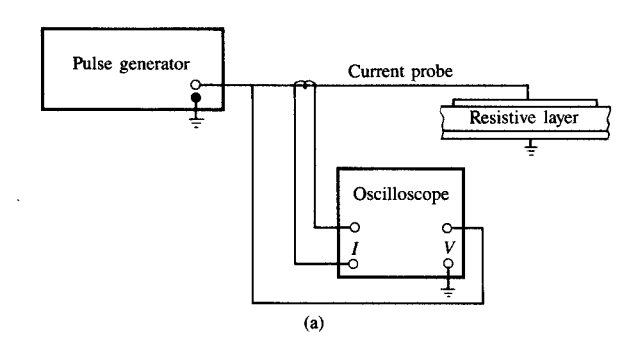
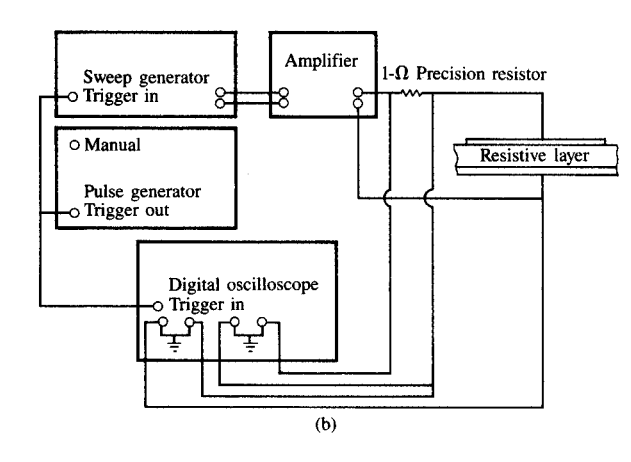


Figure 1

Schematic diagram of a resistive ribbon for thermal transfer printing.





Schematic diagrams of equipment for current-voltage measurements: (a) for pulse measurement; (b) for single voltage ramp measurement.

These Au dots were deposited by sputtering, using silicon masks which were fabricated by an anisotropic etching technique.

• Measurement technique

Current-voltage characteristics were obtained using voltage ramps with time durations of a few to several hundred microseconds. Since changes in characteristics could occur under high-current conditions, single-ramp events were used, and the current and voltage data were recorded using a digital oscilloscope.

An alternative technique used was the application of a series of brief pulses of increasing amplitude to sweep through the current-voltage response. The voltage pulses could be varied from 1 μ s to 1 ms, but 50- μ s pulses at a repetition period of 13 ms were used for most of the measurements. The duty cycle of the pulses was kept low to minimize the heating of the ribbon during the measurement, so as not to cause change in the characteristics. A schematic diagram of the equipment for the pulse measurement is shown in Figure 2(a). A pulse generator was used to generate the square voltage pulses and the current was measured with a current probe. The voltage pulses and the output from the current probe were measured with a storage oscilloscope, and the resulting I-V curves were displayed on the screen.

For the single voltage ramp measurement, the schematic diagram of the equipment is shown in Figure 2(b). The pulse generator was used to trigger a sweep generator for the generation of single voltage ramp waveforms. The base electrode was biased negatively for all measurements, except where specified to the contrary.

Measurements were made over a range of temperatures from -200°C to 50°C by attaching the ribbon samples to a copper plate that could be cooled by liquid nitrogen and temperature-controlled within a vacuum chamber.

Measurements were performed on samples that had received the metallization layer by evaporation in a large-scale commercial evaporator system and also on samples that had been metallized in a laboratory sputtering system. For the effects to be described below, the method of deposition had a negligible effect on the form of *I-V* curves.

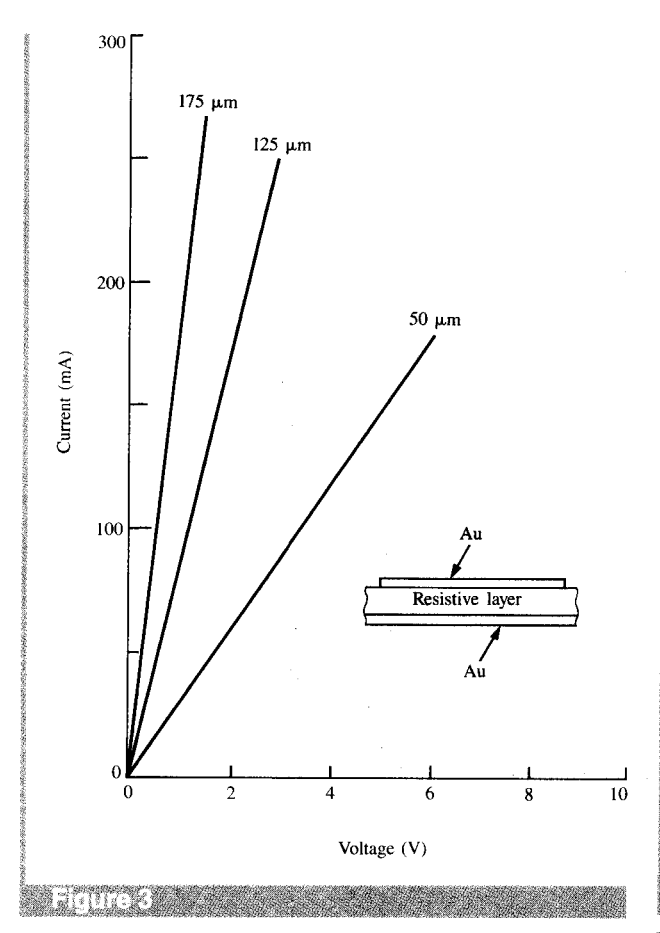
Experimental results—Electrode effects

• Curves using different electrodes

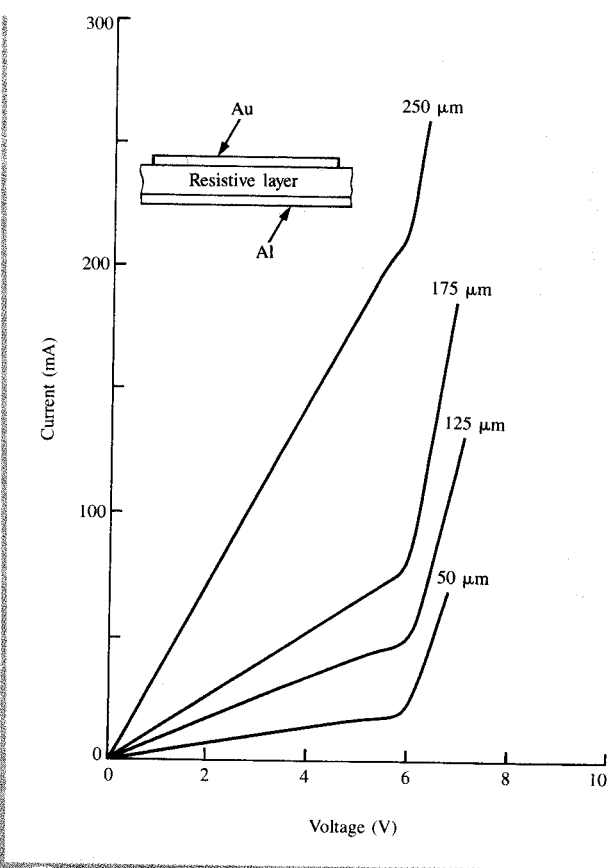
Measurements were performed on four types of samples having

- an Au base contact and Au dot contacts on the upper surface:
- an Al base contact and Au dot contacts on the upper surface:
- an Au base contact and tungsten probe mechanically contacting the upper surface of the polycarbonate layer;
- 4. an Al base contact and tungsten probe mechanically contacting the upper surface of the polycarbonate layer.

As shown in **Figure 3**, the *I-V* curves for the type 1 samples are linear, and the resistance of the sample closely



I-V curves of samples with Au contact on both sides of the resistive layer. The top Au dot size is indicated for each sample.



I-V curves of resistive layer-aluminum interface with top Au dot of differing size.

matches that of the bulk polycarbonate layer. Thus, contact and interfacial resistance are both negligible in these samples.

As shown in **Figure 4**, an interfacial resistance exists between the polycarbonate and Al layers when Al is used as the base contact (type 2). The *I-V* curves exhibit a nearly linear dependence at voltages below approximately 6 V, but the current increases rapidly for voltage exceeding 6 V.

Type 3 samples demonstrated a contact resistance effect, but no interfacial resistance due to the Au base contact. Typical static contact resistance behavior is shown in **Figure 5**.

Type 4 samples displayed both contact and interfacial resistance effects, in addition to the bulk resistance of the polycarbonate layer, as seen in **Figure 6**. This case is closest to the behavior of a ribbon under printing conditions.

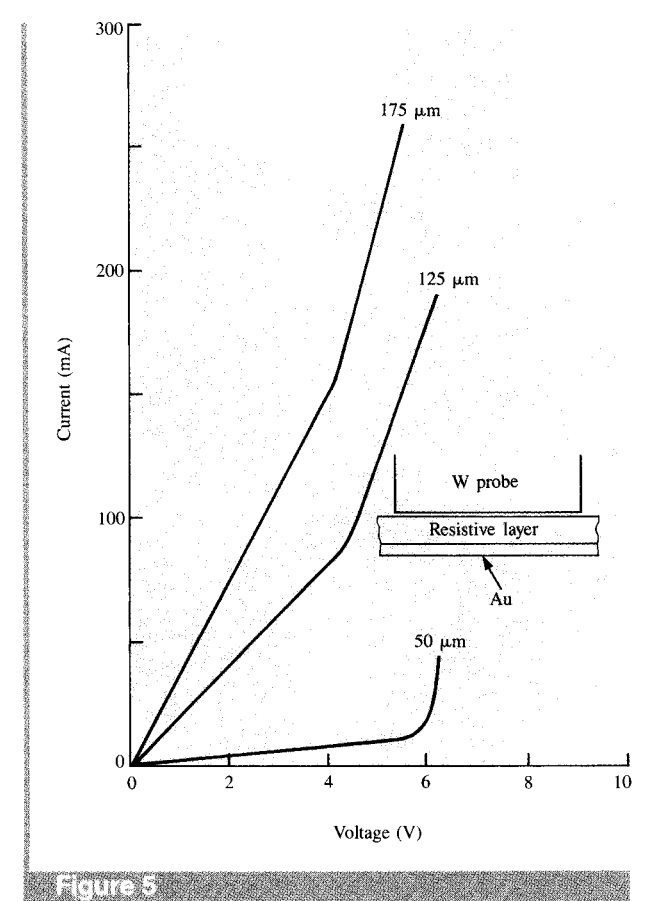
The data from Figs. 3-6 for the 50- μ m top contact are plotted together in **Figure** 7. Curve A corresponds to the bulk resistance of the resistive layer, curve B to the interfacial resistance between the resistive layer and aluminum plus the bulk resistance contribution, curve C to

the contact resistance between the W probe and the surface of the resistive layer plus the bulk resistance contribution, and curve D to the total resistance across the entire ribbon.

At the same current level, if the voltages of curves B and C are added together and the voltage of curve A is subtracted because B and C both contain the voltage drop due to bulk resistance, a new dotted curve B + C - A is produced (Fig. 7). The dotted curve is almost identical to curve D. This result indicates that the total resistance is equal to the contact resistance plus the interfacial resistance and the bulk resistance. For most cases, the bulk resistance is smaller than the interfacial and contact resistance and its value can be ignored. Therefore, the total resistance can be determined from independent measurements of contact and interfacial resistance.

Experimental results—Conduction mechanisms

As can be seen from Fig. 3, the resistive ribbon material behaves in an essentially ohmic manner when measured with deposited gold electrodes. We have studied two resistive ribbons, A and B, with differing resistivity. Sheet resistivity



Static contact resistance measurement with different sizes of W probe for top contact.

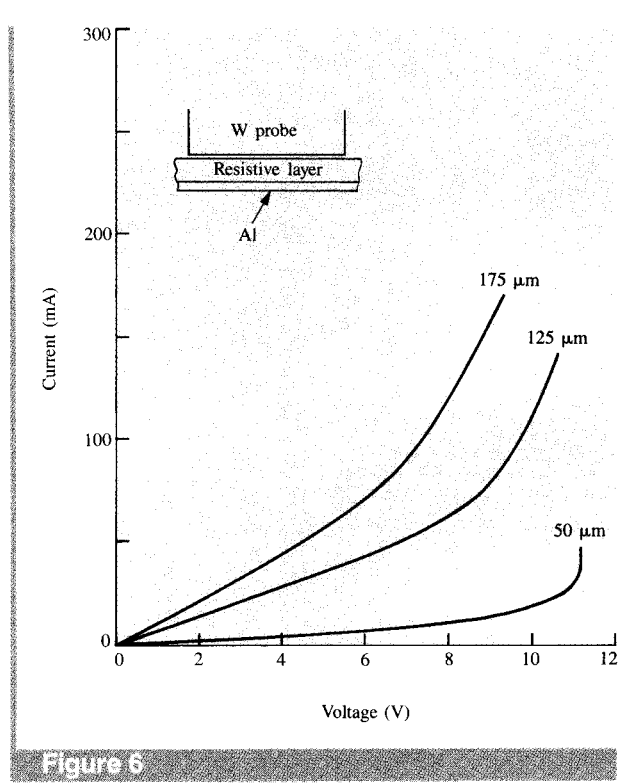
was measured on these two ribbons using Au pads as top contacts with no base contact. The I-V curve, linear to high current densities, is independent of polarity and has only a small change in resistance with temperature at low temperature, as shown in **Figure 8**. Measurements from dc to 1 MHz did not reveal any frequency dependence.

The considerable increase in resistance that occurs when aluminum is used as a contacting layer instead of gold indicates that a barrier exists between the aluminum and the resistive material. Temperature measurements using a gold electrode to eliminate contact resistance and with an aluminum base layer system show that the low field conduction is largely independent of temperature, as shown in **Figure 9**. In this case, the same ribbons A and B were used, with Al as base contact and Au pads as top surface contacts. The low field conduction is ohmic to several volts and is not polarity dependent. It can be noticed in a comparison of Figs. 8 and 9 that the low field resistivity has a temperature dependence that follows very closely that of the resistive medium itself. The significance of this result is discussed below.

At higher fields the current-voltage relationship becomes nonlinear, as described by Cassidy [3]. Experiments have shown that the knee voltage changes only about a volt from -200° C to room temperature, as shown in **Figure 10**. For ramp pulses as short as a few tens of μ s up to a few hundred μ s the nonlinearity shows little frequency dependence and may be retraced repeatedly without change or hysteresis. For longer pulses, or for higher power inputs, the *I-V* curve changes irreversibly to a nearly ohmic resistance, the value of the resistance depending on the voltage applied, as shown below

The results described so far are for the aluminum layer taken as the negative electrode. The effect of taking the aluminum as the positive electrode is shown in **Figure 11**. The *I-V* curve for aluminum biased negatively is shown in the same figure for comparison. It was found that the initial resistance at low voltages is independent of polarity, but the voltage for the onset of nonlinearity occurs at a lower voltage when the aluminum is biased positively. The interface appears to be more fragile when pulsing is done with the aluminum layer as the positive electrode.

Figure 12 shows the result of repeated pulsing experiments on a sample with an Al base contact. First, a single 10-μs voltage ramp was applied to a resistive layer using a 250-μm Au dot for top contact. A low-voltage ramp was applied and



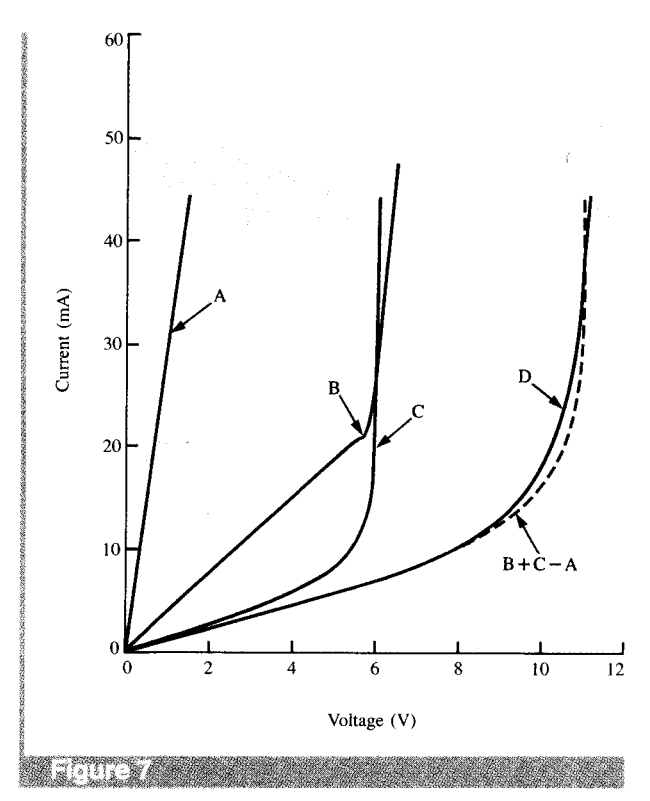
Total static *I-V* measurement with different sizes of W probe for top contact.

the *I-V* curve was recorded; then the voltage was increased to greater than 9 V, as shown in Fig. 12. The *I-V* curves were repeatable up to about 8 V; however, when the applied voltage was greater than 9 V, a new path with lower resistance (dotted line) was observed. This indicated that a permanent change of the properties of the interface had taken place when the high voltage was applied.

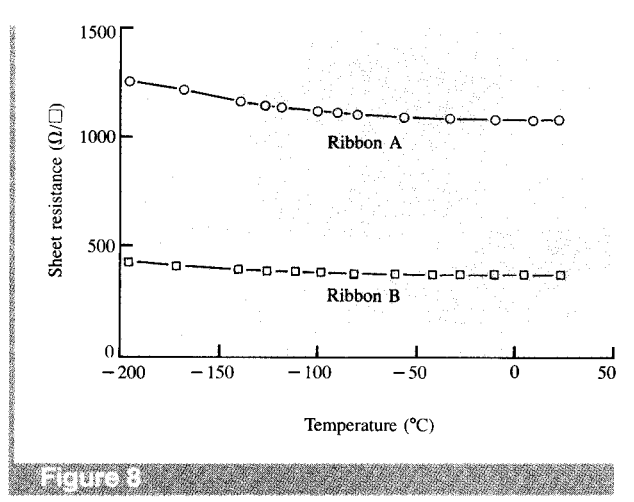
Discussion

Measurements on the resistive medium of the ribbon indicate that the conduction is essentially ohmic to high current densities, with no dependence on polarity and with only a moderate dependence on temperature. Measurements for frequencies from dc to 1 MHz did not reveal any frequency dependence.

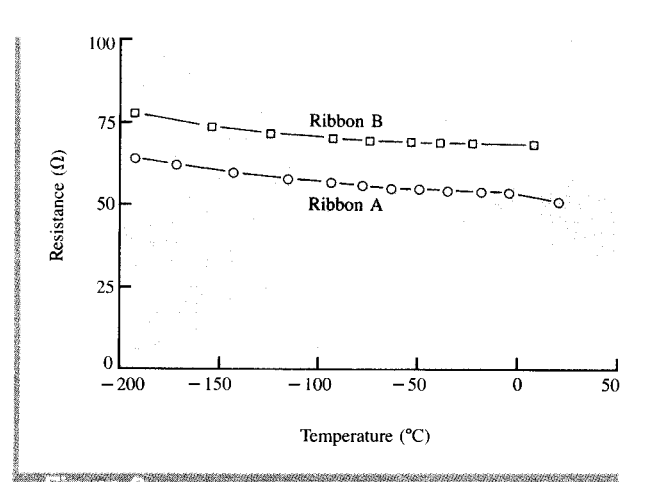
It is of interest therefore to consider the origin of the high resistance and nonlinearity in conduction occurring when aluminum is used as a contact to the resistive material. In view of the ohmic behavior of the resistive material, it is probable that the interface properties are due to the presence of a thin layer of oxide existing at the aluminum-resistive medium interface, rather than to a space-charge barrier as in a semiconductor. As discussed below, this view is consistent with a wide range of data. For voltages up to several volts the interfacial resistance is constant and independent of polarity, showing only weak temperature dependence. This



I-V characteristics from Figs. 3-6 for a 50-μm top contact



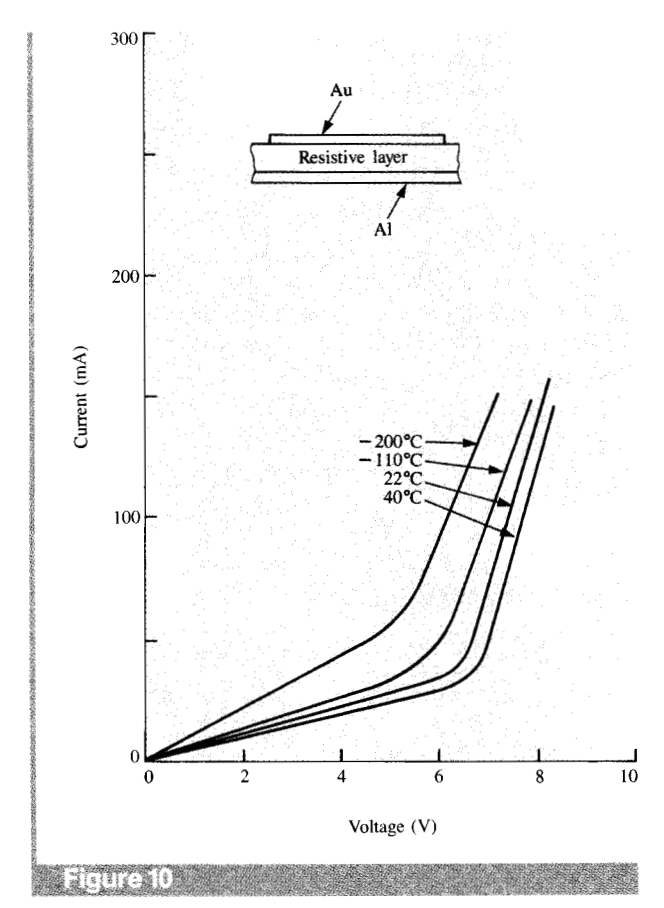
Sheet resistivity as a function of temperature for two ribbons with differing resistivity.



Interfacial resistance as a function of temperature for two ribbons with differing resistivity.

appears to rule out ionic, Schottky, impurity, and space-charge conduction as probable mechanisms for conduction through the thin oxide barrier. A model consistent with all of the above observations is that of conduction via local defects through the oxide, such as pinholes, allowing only a very limited effective area of contact to the resistive medium. The constricted current flow gives rise to an appreciable voltage drop in the vicinity of each defect or pinhole, as described by Holm [4] and shown schematically in Figure 13. The equation for the resistance resulting from an array of such contacts is given by Holm as

$$R = \frac{\rho}{2\pi na} \arctan\left(l/a\right),\tag{1}$$



I-V curve for a ribbon with an Al base electrode and an Au dot top electrode measured over a range of temperatures.

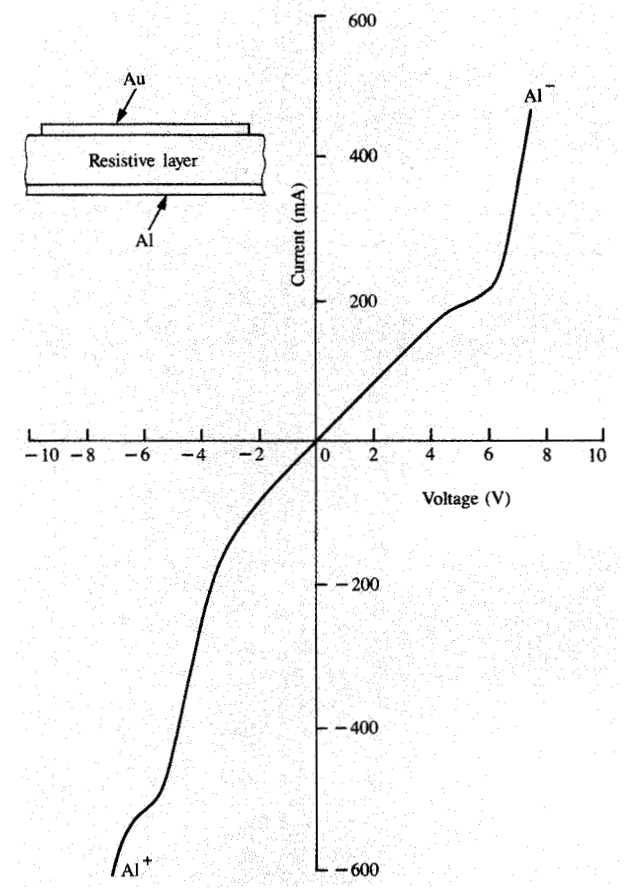
where a is the radius of the microscopic conducting regions and n is the number of such regions per unit area. The mean distance between conducting regions is l, and ρ is the resistivity of the resistive medium. It can be seen that this model explains the observation that the temperature dependence of the interfacial resistance follows closely that of the resistive material.

The observations reported here are consistent with Cassidy's view [3] that tunneling through a thin oxide layer is involved in conduction between the aluminum and resistive medium; however, it seems clear that the initial portion of the *I-V* curve is due to pinhole- or similar defect-controlled conduction and that tunneling controls the onset of nonlinearity. If this initial linear current component is subtracted from the typical measured *I-V* curve, the resulting curve is very similar to a plot of a tunneling characteristic, when this is represented using a linear scale instead of the logarithmic current axis more commonly employed. The weak temperature dependence, polarity asymmetry, and fast nonhysteretic repeatability through the nonlinear region are consistent with the behavior expected for a tunneling process.

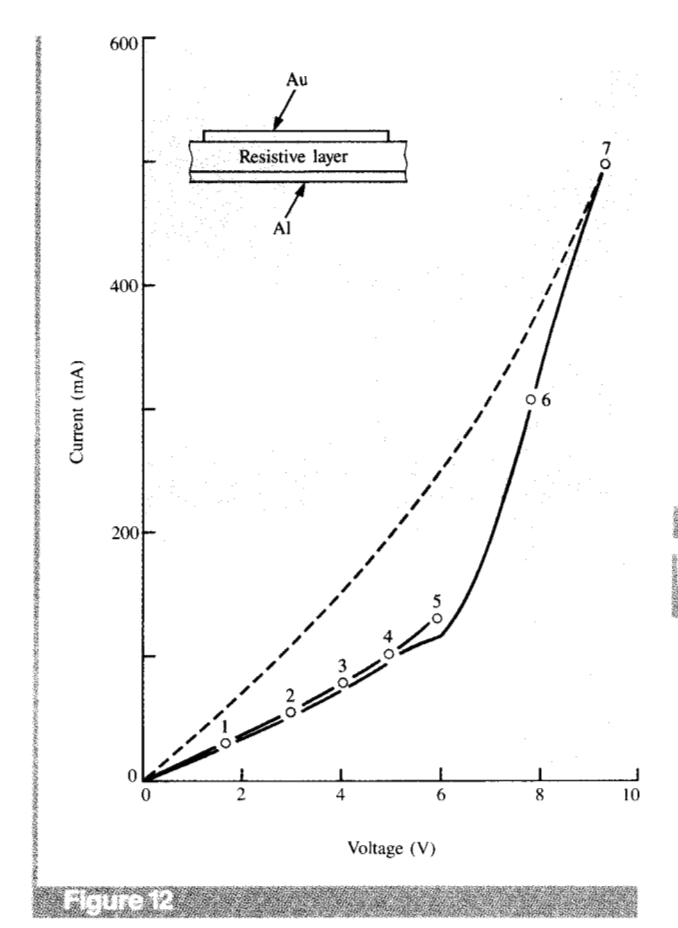
The model developed here shows that at higher fields the oxide barrier becomes transparent due to electron tunneling and gives rise to current flow in parallel with that due to defects.

Simmons has discussed the theory of the electrical tunnel effect for asymmetric junctions, i.e., junctions having electrodes of differing work function [5]. The current flow through the junction depends on the thickness of the insulator and on the difference in work function of the electrodes. The *I-V* characteristic is polarity dependent, with the greater current flowing when the electrode of lower work function is positively biased, as in the present case, where the work function of aluminum is believed to be about 4 eV, while the work function of carbon is about 5 eV [6].

Figure 14 shows a plot of current density (J) versus voltage (V) for several values of oxide thickness using Simmons' equation from Chopra's book [7], tunnel junction with work function of the electrodes ϕ_1 and ϕ_2 taken to be 1 eV and 2 eV on either side of the oxide layer:



I-V characteristics at different polarities for a ribbon with an Al base electrode and a 125-μm top Au contact.

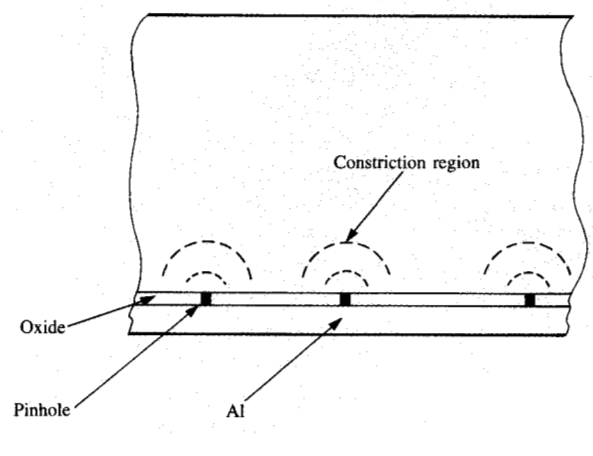


Current-voltage curves measured with repeated single pulse on a ribbon with an Al base electrode and a 250-µm top Au contact.

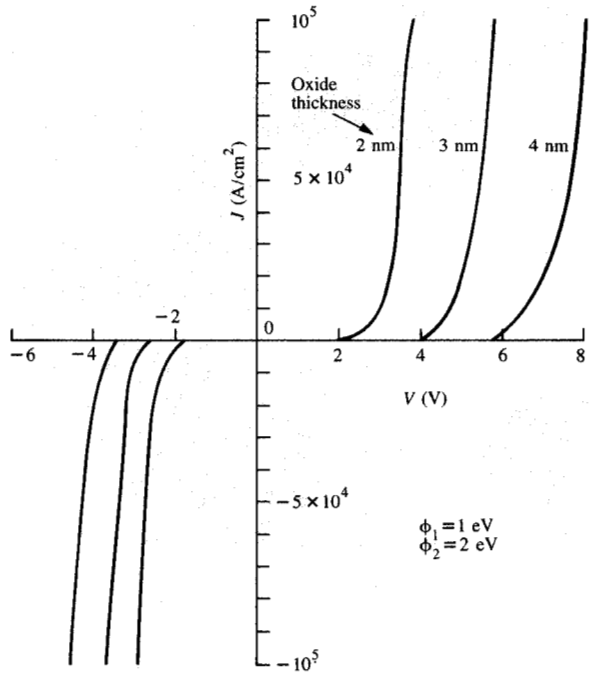
$$J = \frac{6.2 \times 10^{10}}{\Delta s^2} \{ \overline{\phi} \exp(-1.025 \Delta s \overline{\phi}^{1/2}) - (\overline{\phi} + V) \exp[-1.025 \Delta s (\overline{\phi} + V)^{1/2}] \}.$$
 (2)

Denoting the reverse direction current by J_1 (with the electrode of lower work function positively biased) and the forward direction current by J_2 , we obtain, for the voltage range $0 \le V \le \phi/e$, $J_1 = J_2$ by substituting $\overline{\phi} = (\phi_1 + \phi_2 - eV)/2$ and $\Delta s = s$ in Eq. (2). For $V > \phi_2/e$, ϕ_1/e , J_2 is given by using $\overline{\phi} = \phi_2/2$ and $\Delta s = s\phi_2/(eV - \Delta\phi)$, where $\Delta \phi = (\phi_1 - \phi_2)$, and J_1 is given by using $\overline{\phi} = \phi_1/2$ and $\Delta s = s\phi_1/(eV - \Delta\phi)$. Thus J_1 is not equal to J_2 ; that is, the junction is rectifying. In the present case, however, the low-current behavior is dominated by the defect conduction process.

The sharp onset of current can be noted, and the voltage at which the onset occurs is approximately proportional to oxide thickness as expected (Fig. 14). This plot illustrates the expected behavior of tunnel current for the parameters chosen; however, more work is needed to establish in detail the correlation between this model and the resistive ribbonaluminum interface behavior.



Constriction current model



Theoretical tunnel current characteristic from Simmons' equations.

Summary

It has been shown that by proper choice of electrodes, the electrical effects within the ribbon, due to contact resistance beneath a mechanical probe, to bulk conduction within the resistive medium of the ribbon itself, and to the aluminum base layer, may be studied separately. The resistive medium

is an ohmic conductor with a resistivity of approximately 0.6 Ω -cm, and commonly the voltage drop across the ribbon may be largely due to the mechanical probe and aluminum layer interfaces.

In particular, the data support the hypothesis that a layer of oxide develops at the aluminum-resistive medium interface. The interfacial resistance observed at voltages up to several volts is consistent with conduction through microscopic conducting regions through the oxide, which gives rise to current constrictions within the resistive medium. This resistance is therefore a measure of the quality of the oxide rather than of its thickness. On the other hand, the *I-V* nonlinearity arises from additional current flow through the oxide, in a manner qualitatively as expected for a tunneling process. In this case, the voltage for onset of nonlinearity is expected to be approximately proportional to oxide thickness and is apparently determined by the naturally terminating growth of the native oxide.

If, however, too high a power level is sustained across the ribbon, irreversible changes occur, producing a reduction of the initial resistance to a value determined by the voltage applied.

The present studies have provided a basis for establishing a model for the major electronic processes occurring in the resistive ribbon which is in agreement with a wide range of data.

Acknowledgments

The authors wish to thank E. G. Lean for his advice and encouragement, D. McClure for collaboration with some of the experiments, and J. R. Crowe and N. Paynes for the deposition of the thin films.

References

- L. Montanari and F. Knirsch, "Electro-Thermic Printing Device," U. S. Patent 3,744,611 1973.
- K. S. Pennington and J. L. Mitchell, "Improved Print Head and Ribbon Structure for Thermal Transfer Printing Application," Research Report RC-5878, IBM Thomas J. Watson Research Center, Yorktown Heights, NY, 1976.
- B. Cassidy, "Ribbon Electrical Characteristics in the High Current Region," Information Products Division, Lexington, KY, unpublished work.
- R. Holm, Electric Contacts, Springer-Verlag Inc., New York, 1967.
- J. G. Simmons, "Electrical Tunnel Effect Between Dissimilar Electrodes Separated by a Thin Insulating Film," J. Appl. Phys. 34, 2581 (1963).
- Handbook of Chemistry and Physics, 59th Edition, CRC Press Inc., Cleveland, OH, 1979.
- K. L. Chopra, Thin Film Phenomena, McGraw-Hill Book Co., Inc., New York, 1969.

Received October 14, 1984; revised April 26, 1985

Derek B. Dove *IBM Research Division, P.O. Box 218, Yorktown Heights, New York 10598.* Dr. Dove attended the Imperial College of Science and Technology, London, England, receiving the Ph.D. degree in 1956. After several years working on radioisotopes at A.E.R.E., Harwell, he joined the Bell Telephone Laboratories and was involved in studies of the structure and magnetic properties of thin films. In 1967 he became a professor of materials science and electrical engineering at the University of Florida, Gainesville, and in 1977 joined IBM at Yorktown Heights as a manager in the display and printing area, where he has worked on electroluminescence, phosphors, and, more recently, resistive ribbon printing.

Kwang Kuo Shih IBM Research Division, P.O. Box 218, Yorktown Heights, New York 10598. Dr. Shih is a research staff member in the I/O Department at the Thomas J. Watson Research Center. He received his Ph.D. in electrical engineering from Stanford University in 1966. His research interests include device physics and materials. Dr. Shih has received an IBM Outstanding Contribution Award and six IBM Invention Achievement Awards.